Jpn. J. Appl. Phys. Vol. 34 (1995) pp. 3298–3302
Part 1, No. 6A, June 1995

Analysis of a Laser-Cooled Mach-Zehnder Atomic Interferometer

Tetsuya MUKAI and Fujio SHIMIZU

Department of Applied Physics, University of Tokyo, Bunkyo-ku, Tokyo 113, Japan

(Received January 17, 1995; accepted for publication March 18, 1995)

Characteristics and operating conditions of an atomic Mach-Zehnder interferometer are discussed. It is shown that a laser-cooled ultracold atomic source and detection of interference by spatially resolved detector greatly improve the performance of the atomic interferometer.

KEYWORDS: interferometer, atom, rare gas, metastable state, grating, beam splitter, grating deflector, Moire pattern, electrostatic deflector, atomic beam intensity

1. Introduction

An interferometer is a device that measures a small displacement of length with accuracy corresponding to the wavelength used. Optical interferometers have existed for more than a century and are used in various fields of science and technology. Electron and neutron interferometers were also invented some 20 years ago. However, an interferometer that uses particle waves of more complex structure, such as atoms and molecules, was realized only within the last few years.[1-6] There are several reasons that hindered the realization of an atomic interferometer. First, the wavelength of an atomic wave is extremely short. The de Broglie wavelength of an atom at room temperature is on the order of atomic size. Second, it is difficult to construct high-quality interferometric components. A standard interferometer requires beam splitters and deflectors. Since atoms do not have charge, it is not possible to manipulate them using Coulomb and Lorentz forces as we do electrons. The strongest electro-magnetic forces on neutral atoms are magnetic dipole force, optical dipole force or the second-order Stark effect. All of these produce a perturbation potential of at most a few kelvins. Since atoms do not pass through a crystal, it is also not possible to manipulate atomic motion by Bragg diffraction in crystals as is used in neutron interferometers. Third, the flux of an atomic beam is many orders of magnitude smaller than that of an optical beam.

In spite of these difficulties an atom interferometer appears promising as an extremely sensitive metrological instrument. The gyroscope is an example. The phase shift caused by the Sagnac effect is

$$\phi = 4\pi\Omega Smv/(hv) = 2m\Omega S/\hbar,$$

where S is the area of the interferometer, m the atomic mass and Ω the angular velocity of the frame. This value is $mc^2/(\hbar\omega)$ times larger than the phase shift of an optical interferometer of equal size. Another example is an accelerometer. A rectangular atomic interferometer with length L can produce the phase shift of

$$\phi = maL^2/(\hbar v),$$

where a is the acceleration of the frame. An atomic interferometer at room temperature with the area of 1 m^2 will produce the phase shift of 2×10^7 rad due to gravity.

An atomic interferometer detects many other quantities undetectable by other interferometers. Atoms are influenced by various kinds of perturbing potentials. Since it takes a fraction of second for an atom to move through the interferometer, an average potential difference of 1Hz causes phase shift on the order of one radian. Therefore, the device is extremely sensitive to interatomic potentials and magnetic and electric field perturbations.

Atoms have an infinite number of internal quantum states, whereas photons, electrons or neutrons have only two degenerate internal states. This enables us to utilize coherent transition between two internal states in beam splitters and deflectors. The transition is accompanied by the absorption and emission of photons, and the atomic path is modified by the momentum of the photon. This technique relates the optical frequency to mechanical quantities such as momentum. Since the frequency is a very accurately measurable quantity, this enables us to calibrate mechanical quantities with a more accurate frequency standard.

To date two kinds of atomic interferometers have been demonstrated. The first is a direct analogy of optical interferometers.[1-3] The second uses coherent resonant light for the division and deflection of the atomic beam.[4-6] Although the first type has a wider range of applications, low atomic flux density and quality of mirrors and beam splitters limit its usage. Beam splitters and mirrors of transparent gratings are relatively inefficient. Deflection by electromagnetic forces is efficient, but rather inaccurate. In this paper we discuss characteristics of the first type of interferometer and propose methods of improving its performance.

2. Atomic Source

Since atomic flux density is one of the major obstacles to achieving high performance, let us first discuss the fundamental limitation of the atomic beam flux available for an interferometer. Photons do not directly interact with each other. In an optical interferometer, the maximum optical power is limited only by the strength of optical components. This limit can be as high as 10 MW/cm^2. In contrast, atoms in an atomic beam strongly interact with each other. An atom in the beam collides at an average distance of $l = 1/(\sigma n)$ and loses its coherence, where σ is the inelastic collision cross section. Therefore, to obtain a large flux the beam diameter must be large. However, in a standard interferometer the wave must be coherent over the entire cross section of the beam. Since we do not have the means to produce

stimulated emission of atoms, the coherent beam must be produced by diffraction of the atomic wave function through a pinhole. When the diameter of the pinhole is d, it diffracts at the angle of

$$\theta_{\mathrm{coh}} = \lambda_{\mathrm{dB}}/d = h/(mv_0 d), \tag{1}$$

where λ_{dB} is the de Broglie wavelength of the atom and v_0 the average velocity of the atom in the reservoir. It is immediately clear from the above discussion that the largest flux of coherent atoms is obtained if atoms are collected from all directions to the reservoir of diameter d, and released immediately. When the incoming flux is sufficiently large, the atomic density n in the reservoir is determined by collision loss in the reservoir. Since the atom travels a minimum distance of d in the reservoir, this is $n = 1/(\sigma d)$. The coherent flux of atoms F_{coh} is the product of the total flux coming out of the reservoir nv_0d^2 and the coherent solid angle θ_{coh}^2.

$$F_{\mathrm{coh}} = nv_0 d^2 \theta_{\mathrm{coh}}^2 = \frac{h^2}{m^2 d(\sigma v_0)}. \tag{2}$$

For a laser-cooled rare-gas atom in $1s_3$ metastable state the above number is 10^3 s^{-1} with $\sigma v_0 = 10^{-16}$ m^{3}s^{-1}. The collision rate of alkali atoms is approximately 2 orders of magnitude smaller, being 10^5 s^{-1}, which is still many orders of magnitude smaller than the flux of photons in a conventional interferometer.

The scheme discussed above can be realized[3] if we cool and trap atoms, and then release them by some means. Rare-gas atoms (Ne, A, Kr and Xe) have an ideal internal level structure for this purpose. Relevant energy levels are shown in Fig. 1.[7-9] The ground state is a $J = 0$ ($1p_0$) state. The lowest excited state has four fine structure levels, which are approximately 10 eV above the ground state. Two of the four levels are metastable levels, of which one has $J = 2$ and the other $J = 0$. The remaining two levels have $J = 1$ and are optically connected to the ground state. The next excited state has ten fine structure levels. The second lowest level has an angular momentum of 3, and is strongly coupled to the $J = 2$ metastable level. Since the $J = 3$ level is not coupled by dipole moment to any other levels, this transition is a closed transition, and we utilize it for the cooling and trapping of rare-gas atoms.[10] We transfer the atoms in this closed transition cycle to the second $J = 0$ metastable state, by first pumping the atom to an upper $J = 1$ level and then letting it spontaneously decay to the $J = 0$ metastable level. Since the $J = 0$ atoms are not influenced by the trapping lasers, or by the magnetic field of the magneto optical trap, they start to fall vertically under gravity. We focus the transfer laser into the trap. Therefore, the source is slitlike. If the laser is directed vertically, it is also considered to be a point source.

Laser cooling increases the number of available atoms as is seen from eq. (2). The lower velocity also increases the de Broglie wavelength, making it easier to manipulate atomic motion. The metastable rare-gas atomic beam described above has other attractive characteristics. It is a scalar particle wave. In addition, metastable atoms are detected with high efficiency by particle-counting detectors such as an electron multiplier and a position-sensitive microchannel plate detector (MCP).

3. Configuration of the Interferometer

Figure 2 shows the Mach-Zehnder interferometer[2] of which characteristics are analyzed. Since we release atoms from a trap, it is convenient to align all components vertically to maintain the symmetry of two atomic paths under gravity. The atomic source S has a lineshape, and can be placed either vertically, or horizontally and parallel to the grooves of a beam-splitting grating G1. The grating G1 is placed below the source separated by the distance l_0. The function of the grating is to produce a discrete change in the horizontal velocity of atoms by

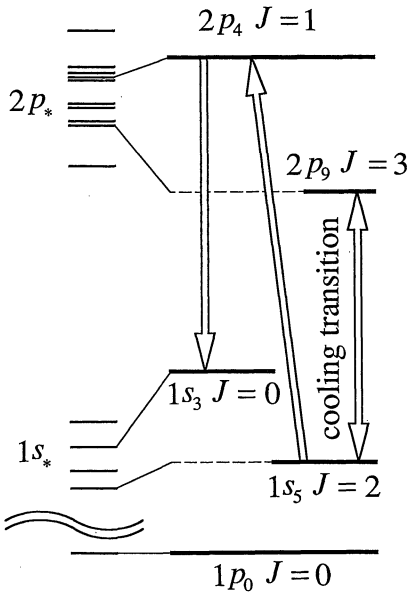

Fig. 1. Energy levels of rare gas atoms relevant to the atom interferometer. Kr and Xe have a slightly different order in the fine structure levels.

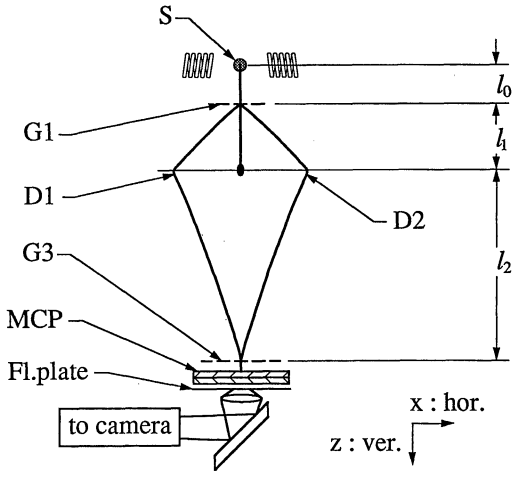

Fig. 2. Configuration of the interferometer. S: the beam source, G1: the first beam splitter, D1 and D2: deflectors, and G3: the matching grating or the second beam splitter.

$$v_\perp = Nh/(mp_1),$$

where N is the order of the diffraction, m the mass of the atom and p_1 the pitch of the grating. It splits the incoming beam into several beams with different diffraction orders N. If the ratio between the slit width d and p_1 is larger than 0.3, the majority of atoms are deflected to $N = 0, 1$ or -1. We select two beams of different orders having the horizontal velocities of $v_{\perp 1}^{(1)} = N_1^{(1)}h/(mp_1)$ and $v_{\perp 1}^{(2)} = N_1^{(2)}h/(mp_2)$. Two deflectors, D1 and D2, are placed at a distance l_1 below G1. They reverse the horizontal velocities of two beams, (1) and (2), to $v_{\perp 3}^{(1)}$ and $v_{\perp 3}^{(2)}$, so that these overlap each other at the second matching grating G3 that is placed at a distance l_2 below the deflectors. Two overlapped beams produce a standing wave pattern above the grating G3, whose pitch $p_3^{(b)}$ is inversely proportional to the horizontal velocity difference

$$p_3^{(b)} = \frac{h}{m\left|v_{\perp 3}^{(1)} - v_{\perp 3}^{(2)}\right|}.$$

Positions of the peaks and valleys of the standing wave interchange as the path length of one beam changes by half the de Broglie wavelength. When the pitch p_3 of G3 is equal to $p_3^{(b)}$, the grating G3 functions as a matching filter. The transmitted beam shows the intensity variation synchronous with the shift of the standing wave position. If the wavefront of the atomic beam is planer, one may use the grating G3 as the second beam splitter in the Mach-Zehnder interferometer. In this case the detector is placed at a distance where each diffracted wave is separated in space.

The heights of the deflectors, D1 and D2, must be adjusted so that two beams overlap on G3. This condition is

$$\left|v_{\perp 1}^{(1)} - v_{\perp 1}^{(2)}\right| t_1 = \left|v_{\perp 3}^{(1)} - v_{\perp 3}^{(2)}\right| t_2,$$

where t_1 is the transit time of the atom from G1 to D1 or D2, and t_2 the transit time from the deflectors to G3.

4. The Beam Splitter

We consider a conventional transparent grating for the beam splitter which was first used by Keith *et al.*[2] The grating pitch they used for their thermal atomic beam was on the order of 100 nm. For cooled atoms a larger diffraction angle is obtained with a larger pitch. This enables use of a grating with a larger area. The efficiency of the grating beam splitter is determined from the relative width of the slit. When the diffraction angle is small, the fractional intensity of the n-th diffracted wave is given by[11]

$$\frac{\left|\int_{-d/2}^{d/2} \exp\left(2in\pi\frac{x}{p}\right) dx\right|^2}{\sum_{n=-\infty}^{\infty}\left|\int_{-d/2}^{d/2} \exp\left(2in\pi\frac{x}{p}\right) dx\right|^2} = \frac{\sin^2(nx)}{\pi n^2 x}, \qquad (3)$$

where $x = \pi d/p$. One can use zeroth- and 1st-order diffracted beams, or two 1st-order beams. Since the transmission of the grating is d/p, the flux of the 1st-order beam is proportional to $\sin^2(nx)$. Therefore, the 1st-order beam flux is maximum when $d/p = 1/2$. With this value the fractional ratios of the zeroth- and 1st-order beams are $1/2$ and $2/\pi^2$, respectively. This means that at best only 10% of the incoming beam is diffracted to 1st-order. Figure 3 shows the fractional intensity of zeroth- and 1st-order beams as a function of d/p.

An alternative method is to use a phase grating,[12] which is realized with an optical standing wave at close resonance. The pitch of the grating is half the optical wavelength, and the phase shift is $\phi_G = \Omega^2 t_{\rm tr}/\Delta\omega$, where $\Delta\omega$ is the detuning of the optical frequency from the atomic resonance, $\Omega = \mu E/\hbar$ the Rabi frequency of the transition and $t_{\rm tr}$ the transit time of the atom through the interaction region. The quality of this beam splitter is limited by the loss due to spontaneous emission, whose probability is approximately $\Omega^2 t_{\rm tr}/(\Delta\omega^2\tau_{\rm nat})$, where $\tau_{\rm nat}$ is the natural lifetime of the transition. Since $\phi_{\rm G} = \pi$ for the phase grating, the probability of spontaneous loss is $\pi/(\Delta\omega\tau_{\rm nat})$. Therefore the loss will become negligible if the detuning is much larger than the natural linewidth. However, larger detuning increases the laser power required to obtain the phase shift of π.

5. Deflectors

Gratings are attractive for use as a deflector that matches the diffraction angle of the grating beam splitter, because the horizontal velocity change is a function of the pitch of the grating, and not of the vertical velocity of the atom. If the pitch is p_2, and the $N_2^{(1)}$th- and $N_2^{(2)}$th-order diffractions are used for beams 1 and 2, respectively, the horizontal velocities after the deflectors are

$$v_{\perp 3}^{(1)} = \frac{N_1^{(1)}h}{mp_1} + \frac{N_2^{(1)}h}{mp_2}$$

and

$$v_{\perp 3}^{(2)} = \frac{N_1^{(2)}h}{mp_1} + \frac{N_2^{(2)}h}{mp_2},$$

which are independent of the vertical velocity. There-

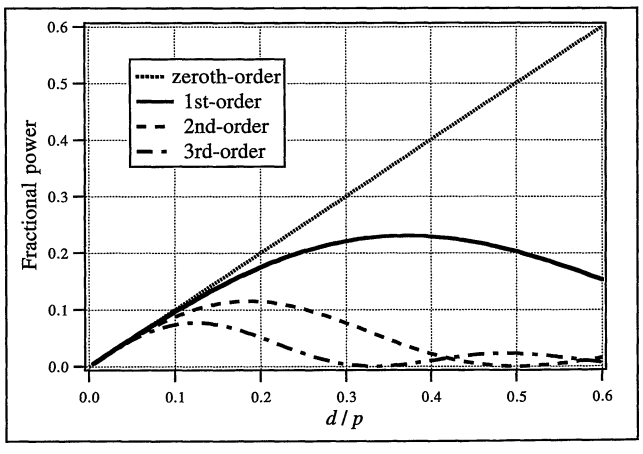

Fig. 3. Fractional power of each diffracted wave of a grating beam splitter as a function of d/p.

fore, the pitch of the standing wave at G3 is velocity-independent. Keith et al.[2] used identical gratings for G1, G2 and G3, and $|N_1^{(1)} - N_1^{(2)}| = 1$ and $N_2^{(1)} = -N_2^{(2)} = 1$. In this case the pitch of the standing wave is equal to that of the gratings.

Because of the low intensity of the atomic beam, it is desirable to use deflectors with higher efficiency. The efficiency of a deflector utilizing static electric or magnetic field gradient is in principle 100%. To produce uniform bending of the entire atomic beam the impulse must be constant along the horizontal direction. Therefore,

$$P = -\frac{1}{v}\int \frac{\partial U}{\partial x} dz = \text{const}, \tag{4}$$

where z is the direction of the atomic beam and x the direction perpendicular to the grating grooves and z. For an atomic beam with $J = 0$, both Stark and Zeeman effects are quadratic, and it can be proven that the above condition cannot be satisfied. A simple proof is given in the appendix. Therefore, when two beams meet at the matching grating G3, the pitch of the standing wave pattern produced by the two beams is not uniform. This will prevent the observation of the interference, if the entire beam intensity is detected by a single detector. However, the mismatch between the interference pattern and the pattern of the matching grating can be corrected if a detector with spatial resolution is used to image the Moire pattern produced by the grating and the standing wave. The fringe position of the Moire pattern moves by one order, when the position of the interference pattern in front of the second grating moves by one order. Therefore, the phase sensitivity is same as that of direct observation of the interference fringes.

Since a commercial MCP detector has spatial resolution on the order of 10 μm when used in counting mode, the detection of the Moire pattern is not difficult for a cold-beam interferometer. Figure 4 shows an example of the calculated Moire pattern of a metastable argon interferometer. The distances between the first grating and electrode and between the electrode and the second grating are 242 mm and 687 mm, respectively. The velocity at the first grating is 2.5 m/s, and the grating pitch is 2 μm. The cross section of the central electrode is elliptical with long and short axes of 7 and 0.2 mm, respectively. Figure 4(a) shows the case in which two gratings are parallel, and (b) that in which they are misaligned by 1°. In either case, the pitch of the Moire pattern is sufficiently wide and a standard MCP detector can resolve the pattern.

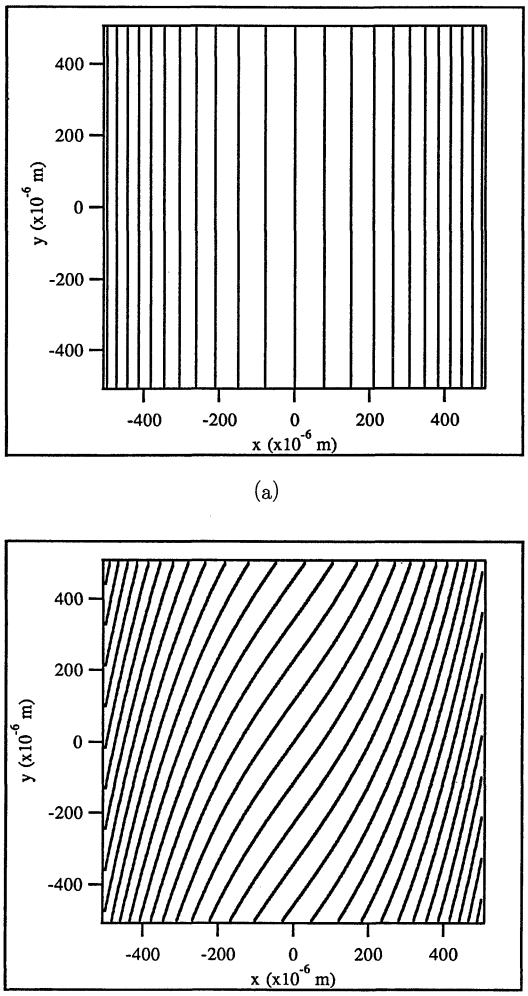

Fig. 4. Calculated Moire pattern, (a) when the alignment of G3 is perfect, (b) when the grating and the standing wave are misaligned by 1°. The lines show the maxima of the Moire pattern.

6. Stability and S/N of the System

There are several factors which must be considered when analyzing actual performance of the interferometer. They may be classified into two categories, namely temporal and spatial effects. Let us first discuss the temporal problem. This arises from the velocity distribution of the atomic source. Since many components are velocity-dependent, the velocity spread degrades interference patterns. However, in the present configuration, atoms have minimum velocity at the source and are accelerated by gravity while they pass through the interferometer. This reduces the relative velocity spread $\Delta v_3/v_3$, and hence the dispersion of interference fringes, where v_3 is the vertical velocity at G3. As was explained in §3, the transverse velocity change at G1, $v_{\perp 1}^{(i)}$, is independent of the vertical velocity of the atom. However, the transverse velocity change at the deflector is velocity-dependent, if the static field deflector is used. The horizontal impulse $m(|v_{\perp 1}^{(i)} - v_{\perp 3}^{(i)}|)$ at the deflector is proportional to the transit time of the atom through the deflector, and therefore inversely proportional to the vertical velocity v_2 at D1 or D2. The relative spread of the standing wave at the matching grating G3 is

$$\frac{\Delta\left|v_{\perp 2}^{(1)} - v_{\perp 2}^{(2)}\right|}{\left|v_{\perp 2}^{(1)} - v_{\perp 2}^{(2)}\right|} = \frac{v_0^2}{4g(l_0 + l_1)}\left|\frac{v_{\perp 1} - v_{\perp 2}}{v_{\perp 2}}\right|,$$

where we used $v_{\perp i} = v_{\perp i}^{(1)} - v_{\perp i}^{(2)}$. Since the velocity spread is compressed while the atom is accelerated due to gravity, this quantity is usually small. For an argon atom cooled to the Doppler limit of 200 μK, at the distance of $l_0 + l_1 = 1$ m, $\Delta v_2/v_2 \approx 5 \times 10^{-3}$. Therefore, approximately 10^2 fringes from the center will be visible.

For a grating deflector, the velocity dispersion does not cause any change because the transverse impulse is determined by the pitch of the grating. Although the efficiency is low, this dispersionless character of the interference fringe pattern is a distinct advantage over static field deflectors.

The spatial problem has two origins. One is the lack of adequate atom-optical components. In Fig. 2 the wavefront at G1 is spherical, which distorts the interference pattern on G3. However, this kind of distortion can be corrected by the observation of Moire pattern.

The other origin is the size of the beam source, which limits the spatial coherence of the atomic beam. In an optical interferometer the entire optical beam is normally coherent. If we apply the same condition in the present case, the diameter D of the first grating G1 must be entirely covered within the coherent solid angle θ_{coh}^2. Using eq. (1) this condition is

$$D < t_{\mathrm{f}} v_{\perp} = t_{\mathrm{f}} v_0 \theta_{\mathrm{coh}} = \sqrt{\frac{2l}{g}} \frac{h}{md}, \tag{5}$$

where t_{f} is the transit time from the source and G1, and the acceleration due to gravity is assumed to be much larger than v_0. This limits the size of the atomic source to be relatively small. In the example of Fig. 2 it is on the order of 10 μm for the grating G1 of 1 mm width.

As we discussed in §2, the atomic density at the source increases in inverse proportion to the size of the reservoir, if it is limited by collisional loss. In practice the density is often limited by other factors and is constant. In this case the grating size does not affect the total atomic flux, because $\theta_{\mathrm{coh}} d$ is constant. However, the condition of eq. (5) is not necessary for observation of interference. When the interferometer is adjusted properly, the two wave packets of an atom that are divided at one point on G1 will converge on an identical spot on G3, if the classical paths are traced. The wave-mechanical spot size of the atom d_{w} is approximately the minimum diffraction angle θ_{dif} multiplied by the length of the interferometer $l_1 + l_2$, which is

$$d_{\mathrm{w}} \approx \frac{\lambda_{\mathrm{dB}}}{d_{\mathrm{w}}}(l_1 + l_2) \approx \sqrt{\frac{h}{m v_1}(l_1 + l_2)}.$$

One can consider that each area of d_{w}^2 on the gratings functions as an independent interferometer. Therefore, to observe interference it is sufficient that the coherence be guaranteed over the area of d_{w}^2 on G1. If $d_{\mathrm{w}} < D$, the source size d increases by the factor of D/d_{w} and the atomic flux by $(D/d_{\mathrm{w}})^2$. For the interferometer of Fig. 2 $d_{\mathrm{w}} \approx 10^{-4}$ m, and the source size can be increased to 10^2 μm.

7. Conclusions

We have discussed in detail various conditions which should be satisfied when constructing atomic Mach-Zehnder interferometers. We have shown that difficulties arising from misalignment and poor quality of interferometric components can be reduced by using a detector with spatial resolution and by detecting the Moire pattern produced by the standing wave pattern of two atomic beams and a grating. The laser-cooled atomic source and a high acceleration due to gravity also help to produce an atomic beam with better monochromaticity. The low flux density of the atomic beam remains a fundamental obstacle limiting the quality of the interferometric measurement.

Acknowledgement

This work was supported by a Grant-in-Aid from the Ministry of Education, Science and Culture.

Appendix

We prove that a thin perfect deflector cannot be constructed in field-free space. Since static electric and magnetic fields in charge- and current-free space satisfy the same equation, we consider only the electric field. First, let us expand the scalar potential ϕ in powers of x, as

$$\phi = a_0 + a_1 x + a_2 x^2 + a_3 x^3 + \ldots,$$

where a_i are functions of z. Since ϕ satisfies the two-dimensional Poisson equation $\Delta\phi = 0$,

$$a_i'' + (i+2)(i+1) 2 a_{i+2} = 0.$$

Using

$$-\frac{U}{\alpha} = |E_x|^2 + |E_z|^2 = \left(\frac{\partial\phi}{\partial x}\right)^2 + \left(\frac{\partial\phi}{\partial z}\right)^2,$$

and

$$\lim_{|z|=\infty} a_i = 0,$$

eq. (4) is written as

$$\frac{vP}{\alpha} = \int \{4 a_0' a_1' + 4(a_0''^2 + a_1'^2) x + 8 a_0'' a_1'' x^2 + \ldots\} dz.$$

To eliminate the linear term in x, a_0'' and a_1' must be zero for all z, hence, the constant term is also zero. This means that a deflector is perfect only when there is no deflection.

1) O. Canal and J. Mlynek: Phys. Rev. Lett. **66** (1991) 2689.
2) D. W. Keith, C. R. Ekstrom, Q. A. Turchetter and D. E. Pritchard: Phys. Rev. Lett. **66** (1991) 2693.
3) F. Shimizu, K. Shimizu and H. Takuma: Phys. Rev. A **46** (1992) R17.
4) F. Riehle, Th. Kisters, A. Witte and J. Helmcke: Phys. Rev. Lett. **67** (1991) 177.
5) M. Kasevich and S. Chu: Phys. Rev. Lett. **67** (1991) 181.
6) J. Robert, Ch. Miniatura, O. Gorceix, S. Le. Boiteux, V. Lorent, J. Reinhardt and J. Baudon: J. Phys. II (France) **2** (1992) 601.
7) C. E. Moore: *Atomic Energy Levels I* (US Government Printing Office, 1949) Circular of NBS 467.
8) C. E. Moore: *Atomic Energy Levels II* (US Government Printing Office, 1952) Circular of NBS 467.
9) C. E. Moore, *Atomic Energy Levels III* (US Government Printing Office, 1958) Circular of NBS 467.
10) F. Shimizu, K. Shimizu and H. Takuma: Jpn. J. Appl. Phys. **26** (1987) L1847.
11) See, for example, M. Born and E. Wolf: *Principles of Optics* (Pergamon Press, Oxford, 1959).
12) P. E. Moskowitz, P. L. Gould, S. R. Atlas and D. E. Pritchard: Phys. Rev. Lett. **51** (1983) 1336.